PAPER

Check for updates

Photocatalytic abatement of ambient NOx by TiO2 coated solar panels†

Jesse Molar,[a] Pierre Herckes ID *[a] and Matthew P. Fraser[b]

Nitric oxide and nitrogen dioxide (combined, known as NOx) and their contribution to ozone and photochemical smog generation are persistent issues in urban environments. Many technologies have been developed to alleviate this issue, including photochemical transformation. While previous experiments have focused on incorporating photocatalysts into paving and building materials, we report coating glass substrates for the eventual application to solar panels that are inherently positioned to optimize the amount of solar exposure they receive, creating a surface compatible with photocatalytic coatings. As most photocatalyst materials absorb the ultraviolet spectrum outside the light range used for energy production, this approach could enable dual-functionalized solar panels for energy generation and air remediation. Proof of concept testing was conducted to determine the effectiveness of TiO2-based photocatalytic products to oxidize NOx to NO_3^-/HNO3. It was found that the tested TiO2-based photocatalytic products can successfully reduce NOx concentrations by up to 36%. With the success of laboratory proof of concept experiments, field testing was conducted to determine if glass panels coated with TiO2 products can reduce NOx concentrations in environmental conditions. Deionized water washes of the coated glass panels were analyzed through ion chromatography to determine the concentration of NO_3^- formed on the surface of the coated glass panels. Field testing resulted in flux values up to 33 mg of NO_3^- per m^2 per day and an average flux up to 8.8 mg of NO_3^- per m^2 per day, representing an order of magnitude value to evaluate possible large-scale implementation. Utilizing field testing results, scale-up estimations suggest widespread application would have a limited impact on total NOx concentrations. Still, at the local scale, deployment at sites with elevated NOx concentrations could meaningfully improve local air quality.

Sustainability spotlight

Air pollution impacts human health in urban centers worldwide, and our work aligns with the Sustainable Development Goal of making cities and human settlements inclusive, safe, resilient, and sustainable. Specifically, by developing and promoting a passive technology that can be incorporated into a sustainable energy system and continuously utilize solar energy to remove nitrogen dioxide pollution, we will advance improved health for communities in a sustainable approach.

Introduction

The nitrogen oxides NO and NO2, combined, known as NOx, are significant pollutants in urban environments generated from high-temperature combustion processes such as the burning of fossil fuels. NO2 has been shown to cause direct health effects such as lung inflammation.[1–5] Nitrogen oxides are a major contributor to the generation of photochemical smog.[6–8] Due to this, NOx is a regulated pollutant. Multiple technologies and techniques have been developed to decrease NOx concentrations emitted at sources such as automobiles, energy generation, and manufacturing, including catalytic converters[9–11] and selective catalytic reduction.[12–16] However, the issue of NOx pollution and its subsequent effect of photochemical smog generation persists.[17–19] Photocatalytic removal of NOx has been proposed as a potential solution to lower NOx concentrations directly, as evidenced by the many reviews and studies found in them.[20–23] Many photocatalytic materials have been explored to remove NOx, such as TiO2,[24–26] modifications to TiO2,[27–29] Li and La-doped BaTiO3,[30] graphitic carbon nitride,[31–33] Bi-based,[34–36] and zeolites.[37,38]

Titanium dioxide is a photocatalyst that can remove pollutants through oxidation and reduction reactions.[39,40] Many applications utilizing TiO2 as a photocatalyst have been

[a]School of Molecular Sciences, Arizona State University, Tempe, AZ, 85287, USA. E-mail: Pierre.Herckes@asu.edu

[b]School of Sustainable Engineering and the Built Environment, Arizona State University, Tempe, AZ, 85287, USA

developed, including antimicrobial surfaces, soil remediation, self-cleaning coatings, and water remediation.[41–44] Proof-of-concept studies have been completed showing TiO$_2$'s capability to oxidize NO and NO$_2$ to NO$_3^-$ photocatalytically.[45,46] The successful implementation of TiO$_2$-based photocatalytic removal of NO$_x$ in proof-of-concept studies has led us to investigate coating the cover glass of solar panels to remove NO$_x$ during energy generation. In addition to the successful proof of concept studies, attempts have been made to utilize photocatalytic coatings in real-world applications of photocatalytic removal of NO$_x$ with varying success.[47–49] Most of these studies focused on applying TiO$_2$-based photocatalysts to construction materials,[50,51] with photocatalytically active cement applications showing successful removal of NO$_x$ in ambient conditions.[52,53] Larger scale experiments have also been conducted, such as in the Brussels Leopold II tunnel, in which a 160-meter tunnel section was coated with a TiO$_2$-based photocatalytically active mortar.[47] This study found that an upper limit of 2% NO$_x$ removal was achieved in these conditions. The decrease in photocatalytic removal in real-world conditions was due to surface passivation caused by the high pollution environment inside the tunnel. The cover glass of photovoltaic cells may provide a coating surface that can avoid the passivation effect seen in applications that focus on coatings of construction materials.

The photovoltaic panels' cover glass (panels placed on top of solar cells to protect the cells) can be coated with photocatalysts to abate NO$_x$ in ambient conditions. Solar panels have been integrated into urban areas, like parking lots and garages,[54,55] with high localized NO$_x$ concentrations.[56–58] The placement of these solar panels presents a unique opportunity for air remediation. Solar panels are periodically washed to ensure efficient energy generation.[59,60] With the addition of TiO$_2$ coatings, cleaning the surface will also remove NO$_3^-$/HNO$_3$ formed during photocatalysis, increasing the removal of NO$_x$ through photocatalysis.[61] Titanium dioxide has a band gap of 3.2 eV (387 nm), making TiO$_2$ a photocatalyst active when exposed to ultraviolet light. Traditional photovoltaic cells do not effectively utilize the ultraviolet spectrum of light for energy generation.[62] The difference in light utilization between TiO$_2$ for photocatalysis and solar panels for energy production could allow photocatalytic removal of NO$_x$ with minimal impact on the solar system's energy production. Solar panels placed in urban environments are less likely to achieve maximum light harvesting than solar farms in rural areas (although panels placed in urban areas may experience less dust deposition, slightly offsetting this); however, photocatalytic removal of NO$_x$ does not scale linearly with light intensity and does scale with an increase in NO$_x$ concentration.[63] Therefore, while application in rural solar farms could increase the photocatalyst's activation compared to urban areas, the elevated NO$_x$ concentrations in urban areas could allow for equal or greater photocatalytic removal performance.

Many studies have successfully coated TiO$_2$ on glass surfaces to produce transparent, superhydrophobic, anti-reflective, self-cleaning, and/or antifogging glass surfaces.[64–67] The application of self-cleaning and antireflective coatings has shown that

TiO$_2$ can successfully coat the cover glass of photovoltaic cells.[68–70] A potential concern with the coating of the cover glass with photocatalysts is the loss of transmittance of the visible light needed for energy generation. Salvaggio et al. produced a transparent TiO$_2$ coating, achieving <1% loss in transmittance when compared to bare glass,[69] with other studies reporting similar results.[71,72]

In the present study, we evaluated the potential of applying TiO$_2$ photocatalysts to the cover glass of solar panels to create a dual-functionalized system for energy generation and passive ambient removal of NO$_x$. The focus here is on the potential of photocatalytic removal of NO$_x$ using a TiO$_2$-based photocatalyst; therefore, a mixture of laboratory-prepared and commercial TiO$_2$ products was coated onto a glass surface, and the photocatalytic removal of NO$_x$ was tested. This included experiments in laboratory conditions where experiments were conducted in batch and continuous flow to show proof-of-concept results of photocatalytic oxidation of NO and NO$_2$ to NO$_3^-$ by monitoring NO$_x$ concentrations before and after exposure to UV light. Additionally, field testing was conducted using TiO$_2$ applied to glass panels (8 × 12 inches) in which DI water washes were used to collect NO$_3^-$ formed through photocatalytic oxidation. The NO$_3^-$ flux was used to determine the magnitude of photocatalytic removal of NO$_x$ in ambient conditions, with photocatalysts applied to glass surfaces. An extended exposure study was performed in outdoor conditions to investigate the durability of the photocatalyst surface and determine if a decrease in photocatalytic removal occurred through photocatalyst soiling or poisoning. Laboratory and field testing photocatalytic removal were compared through a collection of NO$_3^-$, formed by photocatalytic oxidation, to evaluate the pros and cons of performing photocatalytic removal passively (applied in ambient conditions with solar light) or actively (in controlled conditions using a UV light source). Lastly, to determine if this process could be beneficial as a large-scale remediation method, a scale-up estimation was conducted, using the results of field testing to determine the magnitude of removal that could be expected if the widespread application of TiO$_2$ to solar panel surfaces was performed.

Results and discussion

Laboratory proof of concept

Proof-of-concept experiments were conducted to determine whether the chosen photocatalyst coatings (P25 and FN1 on glass slides) remove NO$_x$ (at concentrations relevant to ambient conditions) when exposed to UV-vis light.

Fig. 1 shows the result of the proof-of-concept testing. In laboratory batch experiments, the FN1 and P25 coatings can successfully oxidize NO to NO$_3^-$/HNO$_3$, effectually removing NO$_x$. The FN1 coating seemed to outperform the P25 coating slightly; however, after performing a two-tailed unequal variance T-test, it was determined that there was no significant difference ($p = 0.11$). On average, NO$_2$ concentrations seemed to have increased for the FN1 ($p = 0.09$) coating during exposure, which suggests that complete oxidation to NO$_3^-$/HNO$_3$ may not occur in some experiments. The difference between the starting
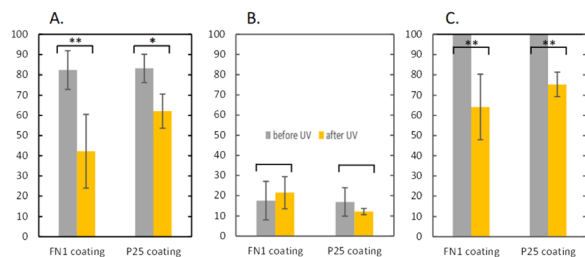
Fig. 1 Proof of concept testing results. (A) NO, (B) NO_2, and (C) NO_x removal. The data was normalized to the starting NO_x concentration. The testing was done in batches, with measurements taken before and after one hour of UV exposure. A UV-vis lamp provided the UV radiation. Concentrations are reported as an average of three runs, and the range of measurements is shown as standard deviation. 2 Tailed paired T-tests were performed to determine the significance in the difference before and after the UV light exposure period for NO, NO_2, and NO_x concentrations, denoted by $*p < 0.05$ and $**p < 0.001$.

Fig. 2 Results from field testing of the photocatalytic removal of NO_x using TiO_2 coatings from March to June 2021: average nitrate formed during exposure. Error bars represent the standard deviation in the amount of nitrate formed. The F-test two-sample variance was calculated for each panel with unequal variance shown between all panels ($p < 0.05$). Two-tailed unequal variance t-tests were conducted for comparison between each panel, and significant differences were found for each case denoted with $*p < 0.05$, and $**p < 0.001$.

normalized NO_x concentration and the normalized NO_x concentration after exposure represents the percentage removal of NO_x. With, on average, 36.9% removal of NO_x for the FN1 coating and 24.7% for the P25 coating ($p < 0.001$). The removal seen here is less than reported in the literature, such as in a study investigating Ag/TiO_2 by Xu et al. in 2017,[73] where ~75% removal was achieved using P25 TiO_2 in one hour. Another study utilizing a SiO_2/TiO_2 mixture achieved up to 90% removal in 15 minutes.[74] However, using different reactor conditions, volumes, and initial concentrations greatly influences these results. Proof of concept testing demonstrated that it is possible to achieve NO_x removal using the photocatalytic P25 and FN1 coatings applied to glass slides under UV-vis light in lab conditions relevant to ambient conditions.

Field testing nitrate flux

To determine whether photocatalytic removal is effective in ambient air with photocatalysts applied to glass surfaces, field testing was carried out in urban Phoenix ambient air with three different photocatalysts applied to 8×12-inch glass panels for a total of four panels (three photocatalysts coated and one control with no coating). Removal of NO_x was measured indirectly by the nitrate formed on the photocatalyst surface generated through the oxidation of NO and NO_2. Nitrate was gathered from the photocatalyst surface by DI water washes and then quantified through IC analysis. The average flux values were calculated for each glass panel over the whole testing period from March to June 2021.

Fig. 2 shows the rate of nitrate deposition at the surface of the glass panels. The control panels' NO_3^- flux is elevated (0.9 mg per m^2 per day) at this urban site, compared to the average rate in the Phoenix area, which was shown to have a dry deposition flux on average of <1.0 kg per ha per year or 0.27 mg per m^2 per day.[75] The elevated NO_3^- on the control panel is possibly due to NO_3^- formed from the adjacent photocatalyst panels; however, this elevated NO_3^- is also seen in another study[76,] where coated surfaces were also placed near the control. Furthermore, this is evidence that each coated surface's NO_3^-
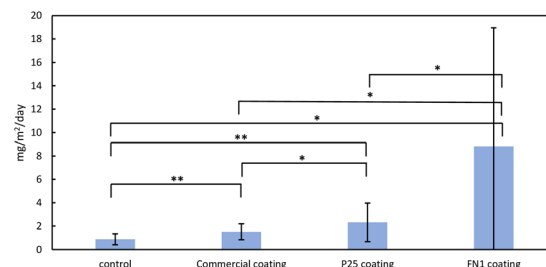
flux may influence the other coated surfaces. During the exposure period, the amount of nitrate formed on the surface of the photocatalyst exceeded the amount of nitrate deposited onto the surface indicated by the control panel (commercial coating $p < 0.001$, P25 $p < 0.001$, FN1 $p = 0.003$). This signifies that NO_x was successfully oxidized to NO_3^-/HNO_3, removing NO_x from the ambient air. The amount of nitrate formed for each photocatalyst varied greatly with FN1, achieving, on average, 8.8 mg per m^2 per day, outperforming the commercial coating, 1.5 mg per m^2 per day ($p = 0.006$), and the P25 coating, 2.3 mg per m^2 per day ($p = 0.01$). The lower performance of the commercial product could be due to differences in the specific surface area and loading area of TiO_2. The commercial product is a proprietary technology, so photocatalyst deposition information is unknown. However, the coating seems to be a thin film almost entirely transparent, suggesting a lower loading of TiO_2 on the surface. This transparency is beneficial for transmitting light through the photocatalyst for energy generation but could result in lower NO_x removal performance.

The nitrate formed on the surface is comparable to another study in which coatings were tested outdoors for 20 months with periodic washing.[76] During this study, two different applications of air-purifying paint were tested. On average, they had 1.76 mg per day for a photocatalytic lime render panel and 3.48 mg per day for a photocatalytic polycarbonate panel, showing that the removal using coated glass panels aligns with these results.

The amount of nitrate formed during exposure varied greatly for all the catalysts, with the FN1 coating showing the most extensive variation. This may be due to changing conditions, such as the NO_x concentrations and humidity. In field testing, an increase in nitrate concentrations collected on the photocatalyst-coated panels compared to the control panel was observed, demonstrating successful NO_x removal in environmental conditions.

Fig. 3 compares light transmission through the FN1 and P25 coated glass panels to a non-coated control. The commercial product was not included in the comparison since it was applied to a different glass product, making the results not comparable to the control.
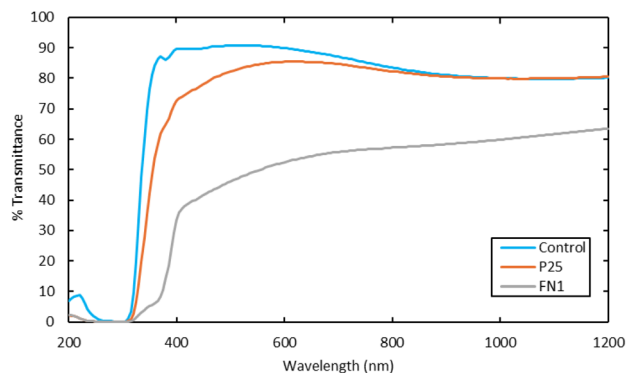
Fig. 3 UV vis transmittance comparing photocatalyst-coated glass to non-coated control.
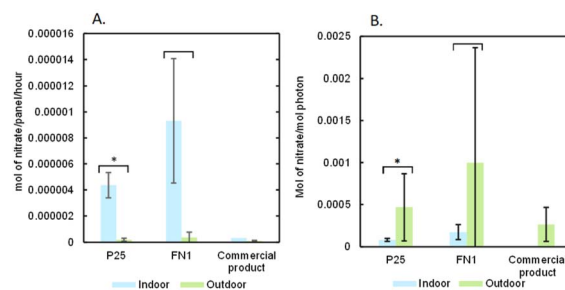

Fig. 4 (A) The nitrate flux comparing the removal of NO_x in the indoor and outdoor experiments. (B) The photon efficiency comparing the indoor and outdoor experiments. The results in both cases are reported as an average, and the error bars denote the standard deviation of the different experiments. The F-test two-sample variance was calculated for each panel with unequal variance shown between all panels ($p < 0.05$). Two-tailed unequal variance t-tests were conducted for comparison between each panel, and significant differences were denoted with *$p < 0.05$. The commercial product was excluded from the t-test analysis because of commercial product indoor testing $n = 1$.

UV-vis transmittance experiments were conducted to determine how much light penetrates the photocatalyst coatings. Light penetration is an important parameter when considering solar panel applications, as even a slight decrease in visible light can significantly reduce energy generation efficiency. Comparing the transmittance of the photocatalyst coatings to the control, the FN1 demonstrated a significant reduction of 20 to 50%, while the P25 coating showed no change to 20%, dependent on wavelength. This decrease in visible light transmission can occur through the photocatalyst coating's absorption or scattering of light. Demonstrating that while the photocatalysts are applied as a thin film and absorb mainly in the UV region of the sunlight and should, in theory, have little effect on the transmission of visible light, in practice, they do affect the amount of visible light that would reach the solar panel. Further tuning of photocatalyst loading would be necessary to optimize the visible light transmission *versus* a potential reduction in NO_x removal.

Comparison between indoor and outdoor removal of NO_x

Photocatalytic removal testing of the glass panels used in field testing was conducted in laboratory conditions to compare removal between indoor (laboratory conditions) and outdoor (ambient conditions) conditions. The results are reported using two metrics comparing NO_3^- formation: NO_3^- flux, which shows the rate of the nitrate formed and photon efficiency, in Fig. 4.

In Fig. 4A, when comparing the rates, the indoor experiments resulted in rates that were an order of magnitude higher than the outdoor experiments for the P25 ($p = 0.003$) and FN1 ($p = 0.23$) photocatalysts. The commercial products demonstrated lower removal in indoor and outdoor experiments when compared to the other photocatalysts. The increased rates for indoor experiments could be due to multiple reasons. The indoor experiments have a higher and more consistent concentration of NO_x in the presence of the photocatalyst during removal (300 ppb of NO) compared to ambient air in Phoenix over six monitoring sites. The average annual mean NO_2 in urban Phoenix is 15.6 ± 5.8 ppb, and the average 1 hour max NO_2 is 55.3 ± 8.4 ppb (**https://www.epa.gov/outdoor-air-**

quality-data/monitor-values-report), which is consistent with for example typical ambient air NO 36.2 ± 59.2 ppb and NO_2 22.8 ± 17.6 ppb in Madrid, Spain.[77] Another significant difference is using the UVA light source in the indoor experiments. When comparing the light source intensity and the solar flux in the number of photons reaching the surface, the UVA lamp outputs three orders of magnitude more photons. In the outdoor experiments, the lower solar photon flux could result in incomplete activation of the photocatalyst, which could reduce removal.

The experiments were also compared using photon efficiency to account for the differences in light sources, as shown in Fig. 4B. The outdoor experiments all exhibited higher photon efficiency when compared to the indoor experiments (P25 $p = 0.009$, FN1 $p = 0.08$), even though the outdoor experiments demonstrated a lower nitrate flux. This is due to the differences between the photon flux in each experiment; the lower photon flux in the UV ranges from solar light resulted in a higher photon efficiency. This leads to the discussion of a trade-off when determining whether to use controlled continuous flow reactors that use a UV lamp or LED as a light source or solar light in ambient removal once pollutants have been released into the ambient air. When conducting removal in a reactor, you can achieve higher removal rates due to complete activation of the photocatalyst, optimal humidity conditions, and consistent mass transfer to the photocatalyst surface. Still, you must consider the cost of the power used to generate UV light to irradiate your photocatalyst. However, with photocatalysts applied to glass surfaces in outdoor locations, such as the cover glass of solar panels, the sun's light can activate the photocatalyst, eliminating the cost of energy usage.

Photocatalyst durability testing

One concern when using a photocatalyst is its durability during extended use, where the removal efficiency could decrease over time.[47,78,79] In Fig. 5, the NO_3^- flux in mg per panel per day is
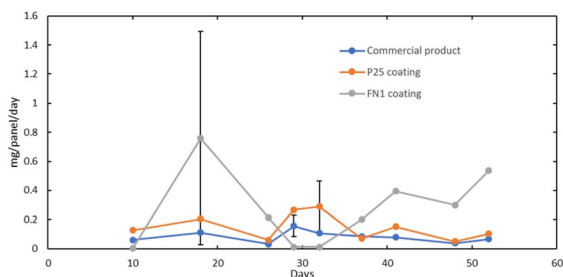
Fig. 5 Results from field testing of the photocatalytic removal of NO_x using TiO_2 coatings from March to June 2021: average nitrate formed during an exposure period. Each data point represents when the photocatalyst-coated glass panel was washed with DI water, and nitrate was quantified using the abovementioned method. The data is reported as a flux of nitrate formation in mg per panel per day. Errors bars represent the relative standard deviation over the entire exposure period for each catalyst (RSDs: commercial product = 47%, P25 = 61%, FN1 = 96%).

shown for the three photocatalytic panels that were tested over the 52-day testing period to determine whether the soiling of the catalyst occurred over the three-month use period. The exposure period for the photocatalyst glass panels varied from 3 to 10 days, with water washing between each period. This variation was done to determine if more extended periods of exposure without washing would result in lower nitrate formation.

In the testing of the photocatalyst-coated glass panels, it was shown that there is no trend of decreasing photocatalyst effectiveness with an increasing number of days of exposure. This demonstrates that photocatalyst passivation does not occur in a quantifiable amount on time scales of up to ten days of exposure. Fig. 5 also shows the nitrate flux of three different photocatalysts using the same coating over 52 days. While there is a considerable variation in the amount of nitrate formed during the duration of field testing, a decrease in the effectiveness of the photocatalyst was not observed. However, the FN1 coating showed wear and tear, and dust buildup on the glass surfaces was observed in visual assessments shown in Fig. 6.

The durability of the photocatalyst coatings is consistent with previous outdoor studies, such as in Luevano-Hipolito and Martinez-de la Cruz, 2018 where TiO_2 was incorporated into

stucco blocks.[61] These blocks were left outdoors for one year and tested indoors monthly for photocatalytic removal. During this, a decrease in photocatalytic removal was observed after three months of not being washed and continued to decrease until the twelve-month point when the blocks were washed with water. After washing, photocatalytic activity was revitalized back to its original effectiveness. Therefore, if occasional washing of the photocatalyst surfaces is conducted, photocatalytic coatings maintain removal efficiency in ambient conditions.

Estimation of maximum removal

The low concentration of NO_x in ambient air could potentially limit the effectiveness of solar panel coatings for NO_x removal. In combination with inconsistent mixing, this suggests that optimal NO_x removal may not be achieved due to insufficient mass transfer to the photocatalytic surface. To understand whether maximum removal is achieved, an average maximum nitrate formed on a photocatalytic surface was calculated.

In Fig. 7, we can see the range of nitrate formed on the surface compared to the total maximum possible nitrate that could be formed on the photocatalytic surface. This comparison shows that the maximum possible nitrate formation related to the removal of NO_x is not achieved during outdoor exposure. This can be explained by insufficient mass transfer to the surface due to the inconsistent mixing in ambient air. In conclusion, the coatings should be placed in an area with an increased NO_x concentration and mixing to increase NO_x removal.

Potential large-scale impact

From the results gathered during field testing, we estimated the effectiveness of the photocatalytic removal using large-scale application. For this exercise, we propose coating all the current photovoltaic cells deployed by Arizona State University. There are 174 664 photovoltaic panels in use by Arizona State University spread throughout multiple campuses. Using the average photovoltaic panel area (1.62 m²), the total area
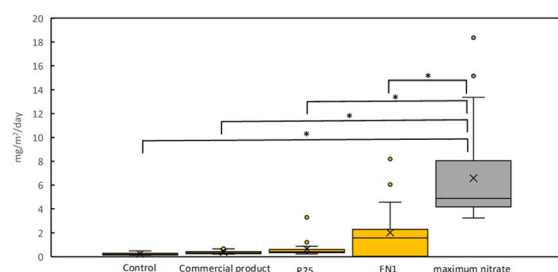

Fig. 7 Results from field testing show nitrate formed on the surface compared to the total possible nitrate formation based on NO_x deposition. NO_x data was obtained off-site from the field testing at a nearby FRM (Federal Reference Methods) site. Data is presented as a box and whisker plot to show the range of data. The dots represent outlier data points. The F-test two-sample variance was calculated for each panel compared to the maximum nitrate with unequal variance between all panels ($p < 0.001$). Two-tailed unequal variance t-tests determined that NO_3^- formed significantly differs from the maximum nitrate denoted by * ($p < 0.001$).

Fig. 6 Image of control panel dust buildup after 10 days of outdoor exposure.

coverage is 283 969 m^2. We will use the highest average removal photocatalyst, the FN Nano FN1 photocatalytic paint, which achieved an average of 8.82 mg per m^2 per day. Scaling up the removal to the area coverage of the Arizona State University's photovoltaic fleet over a year, we calculated, on average, 914 kg of NO_3^- formed annually. Converting this value to NO_2 removal, we would achieve, on average, the removal of 678 kilograms of NO_2 per year. This is roughly equivalent to an offset of 750 car emissions for a year. While helpful, it is not on a scale of removal to be a solution to overall air quality on a city-wide scale. With these results, focusing on a smaller scale and looking at air quality improvement locally in areas such as parking garages would be advisable. Considering the possible cost of coating a large solar fleet like ASU's and offsetting roughly 750 car emissions a year would not be an economical solution. Putting these results in context, in Luevano-Hipolito and Martinez-de la Cruz, 2018 it was reported that TiO_2 integrated into stucco (CleaNO$_x$) could yield up to 256.72 g of NO per year per m^2,[61] assuming an average conversion of NO of 40% with eight hours of light, compared to our study estimation, yielding 2.39 g of NO_2 per year per m^2. This shows two orders of magnitude less removal in this study. However, the methods of estimation differ in a couple of crucial ways; in both studies, the analysis of the removal of NO_x was done indirectly (here quantified by NO_3^- formed). In their research, all NO_x removal measurements were taken under laboratory conditions (controlled humidity, mixing, and UV lamp irradiation) after weathering in outdoor conditions, which could account for higher estimation.

Experimental

Preparation of the catalytic surfaces

The catalyst surfaces were prepared by dip-coating TiO_2 products onto glass slides (20 × 70 mm). Two coatings were prepared: a commercial FN1 photocatalytic[80] paint (specific surface area 35–65 m^2 g^{-1}) and a laboratory-prepared suspension of Evonik Aeroxide P25 particles (specific surface area 35–65 m^2 g^{-1}) (Essen, Germany). The P25 particle coating was prepared using the method described by Tantra *et al.* in 2015;[81] P25 (50 mg) was weighed and placed into a beaker (60 mL). DI water (50 mL) (>18.4 MΩ cm, Purelab Flex, IL, USA) was added to the beaker to create a TiO_2 particle suspension with a 1 mg mL^{-1} concentration. After the P25 dispersion, it was sonicated in an ice bath using the QSonica Sonicator Q500 (Newton, Connecticut) in pulsed operation mode with 80% on and 20% off. The sonicator ran at 20 kHz with a delivered power of 50 W for 15 minutes. Before coating, the glass slides were prepared by washing with DI water (>18.4 MΩ cm, Purelab Flex, IL, USA), left to dry for 1 hour in air, then washed with isopropyl alcohol, and left to dry in air for 1 hour (with a control glass slide prepared using the same method). The glass slides were then dip-coated with a dip coating removal speed of 1 cm min^{-1} in the FN1 and P25 solutions. The glass slides were dried in ambient air at room temperature for 24 hours before testing.

Two sets of four 8 × 12-inch glass panels (0.062 m^2 surface area) (American Glass, Phoenix, AZ) were prepared for field testing. A set of control panels was obtained by using an unmodified glass panel. The glass panels were prepared for coating by washing with DI water (>18.4 MΩ cm, Purelab Flex, IL, USA), left to dry for 1 hour in air, then washed with isopropyl alcohol and dried in air for 1 hour (with control glass panels prepared using the same method). The Aeroxide P25 TiO_2 (Evonik, Essen Germany) and FN1 photocatalytic paint (FN Nano, Prague Czech Republic) panels were coated by pipetting each TiO_2 product (20 mL of 1 mg per mL TiO_2) to coat the surfaces thoroughly (0.32 g per m^2 loading area). The glass panels were placed on a flat surface, and the first 10 mL of photocatalyst was pipetted along the edges of the glass panel, and the following 10 mL was used to fill in the middle of the panel while ensuring complete coverage of the entire glass panel. The glass panels were then dried in ambient air at room temperature for 24 hours. The last set was a prepared proprietary commercial product, where TiO_2 particles were impacted onto a glass surface (referred to as the commercial product).

UV-vis transmittance

Transmittance measurements were conducted for the FN1 and P25 coatings compared to the control panel (non-coated glass panel). The commercial product was not compared because it used a different glass product, making comparison to the control impossible. UV-vis transmittance measurements were performed using a PerkinElmer Lambda 905S (Waltham, MA). Glass panels of 2 × 2 inches were coated using the previously detailed method using 1 mL of 1 mg mL^{-1} of photocatalyst, consistent with the loadings applied to the glass panels used in field testing. Experimental parameters are shown in Table 1.

Laboratory experiments

Photocatalyst testing was carried out using the experimental setup shown in Fig. 8. It consisted of a gas dilution system, a UV-vis light source from the top of the reactor, a rectangular flat plate reactor 12 × 10 × 10 inches (20 L), glass slides (20 × 70 mm) coated with TiO_2 placed in the center and bottom of the reactor, a vacuum pump, and a NO_x analyzer. The UV-vis Newport Oriel Instruments 300 W xenon arc lamp with a 1.5G air mass filter (Newport Oriel Instruments, Irvine, CA) activates the catalyst. Humidity was added to the reactor by bubbling the inlet gas through DI water in a beaker placed in the reactor and maintained at 30 to 40% relative humidity, monitored with a Govee hygrometer/thermometer (Shenzen, China). The NO_x

Table 1 UV vis-transmittance experimental parameters

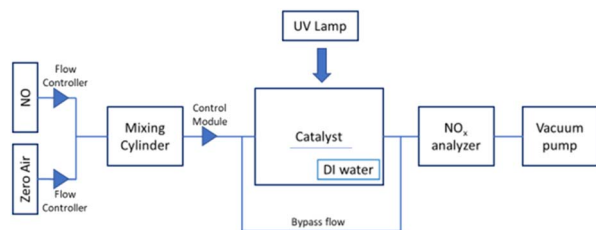| Equipment Name	Perkin Elmer Lambda 905S
Module	140 mm integrating sphere
Data interval	5
Detector response time (s)	0.51
Slit size (mm)	1
Detector change (mm)	800
Lamp change (mm)	200
Mask size (mm)	5
References	uSRS99, SRS99

Fig. 8 Laboratory setup.

concentrations were monitored using a Thermo Environmental Instruments 42C NO, NO_2, NO_x chemiluminescence detector (Waltham, MA) to determine the concentrations within the reactor before and after light exposure.

Proof of concept photocatalytic removal of NO_x experiments were conducted in batch mode for the FN1 and P25 photocatalysts coated onto glass slides. Gas mixtures were provided through a custom-built Alicat mass flow controller gas dilution system (Tucson, AZ). A desired concentration of NO was obtained by mixing NO (Mesa specialty gas 250 ppm, N_2 balance) with zero air (Airgas UHP N_2 78%, UHP O_2 21%) in a mixing cylinder and passed into the reaction chamber, with the chosen photocatalyst in place, until steady state was reached. After a steady state was achieved, NO, NO_2, and NO_x concentrations were recorded, and the reactor was sealed for one hour of light exposure. During the hour of light exposure, the gas mixture was directed through the bypass flow. After the light exposure period, the reactor was unsealed, the resulting gas was directed through the NO_x analyzer, and the NO, NO_2, and NO_x concentrations were recorded. The resulting NO, NO_2, and NO_x concentrations were then normalized to the starting NO_x concentration, and the results were reported as an average over the experiments for the two photocatalysts. This experimental setup deviates from the international standard (ISO 22197–1:2016 – Test method for air-purification performance of semiconducting photocatalytic materials in a couple of key ways: experiments were conducted in batch flow mode, increased reactor volume (20 Liters), larger slit height of inlet gas flow (6 inches).

Field testing

Field testing was carried out on the roof of the ISTB4 at Arizona State University from March to June 2021, with the goal being to use the amount of nitrate formed on the surface during the exposure period to determine if removal is possible in ambient conditions and what magnitude of removal can be achieved. The two sets of photocatalyst panels prepared using the abovementioned method were alternated in exposure periods ranging from 3 to 10 days. After each exposure period, a fresh set of glass panels replaced the recently exposed panels. The exposed panels then received a 10 mL DI water (>18.4 MΩ cm, Purelab Flex, IL, USA) wash, repeated three times to collect the nitrate formed due to the photocatalytic oxidation of NO_x to NO_3^-/HNO_3. The nitrate washes were carried out by pipetting 10 mL of DI water using a glass funnel with the solution collected in a falcon tube. The repeat washes were carried out

using the previously pipetted solution with each round, ensuring the DI water was applied to the entire glass panel surface. The nitrate washes were then filtered using the Millex 33 mm 0.22 μm syringe-driven filter unit (Millipore, Bedford, Massachusetts). The samples were then characterized using ion chromatography to determine the nitrate concentrations after exposure. Anion recovery was measured *via* ion chromatography (Metrohm 930 compact IC Flex, Herisau, Switzerland). A standard anion method was used[66,82] with 3.2 mM sodium bicarbonate ($NaHCO_3$) as the eluent and 0.5 mM sulfuric acid (H_2SO_4)/20 mM oxalic acid as the regenerant solution. Calcium nitrate tetrahydrate (Sigma-Aldrich) 99% was used to prepare standard curves. To better understand the scale of removal achieved, flux values were calculated, showing the amount of nitrate formed during exposure. The rate of nitrate formation was calculated by taking the amount of nitrate removed and normalizing that value to the number of days of exposure and the surface area of the glass panel scaled up to 1 m^2. The data was then reported as an average flux for each instance of DI water washing after the exposure period.

Extended exposure experiments were conducted for each photocatalyst to determine if extended exposure decreased nitrate formation on the surface. The photocatalyst glass panel exposure periods were varied from 3 to 10 days. This variation was done to determine if more extended periods of exposure without washing would result in lower nitrate formation. The testing was carried out using the same photocatalyst-coated panels with periodic DI water washes to determine whether the catalyst soiling occurred over the 52-day use period.

To further understand whether the maximum removal of NO_x, based on the NO_x concentration and deposition rate, is reached, the maximum nitrate formed on a photocatalytic surface was calculated using NO_x concentrations from a nearby FRM site over the field-testing exposure period. Further, a range of the maximum possible nitrate formed using this average NO_x concentration was calculated.

Comparison of indoor and outdoor nitrate flux

Further reactor experiments were conducted to compare outdoor nitrate fluxes to laboratory results using the photocatalyst-coated glass panels used during field testing. These experiments were performed in continuous flow mode, and the above setup (Fig. 8) was used with some changes. A new rectangular flat plate reactor 24 × 12 × 12 inches (56 L) was used to house the photocatalysts applied to the glass panels (8 × 12 inches) shown in Fig. 9. The glass panels were placed on the bottom of the reactor. The FN1, P25, and commercial products were all tested in triplicate. Gas mixtures were provided through a custom-built Alicat mass flow controller gas dilution system (Tucson, AZ) continuously at 2 liters per minute. A desired concentration of NO was obtained by mixing NO (Mesa specialty gas, NO 250 ppm, N_2 balance) with zero air (Airgas, UHP N_2 78%, UHP O_2 21%) in a mixing cylinder and passed through the reactor until a steady state was achieved, with the NO, NO_2 and NO_x concentrations being continuously monitored. A 36 W Cure UV UVA interchangeable Lamp (Cure
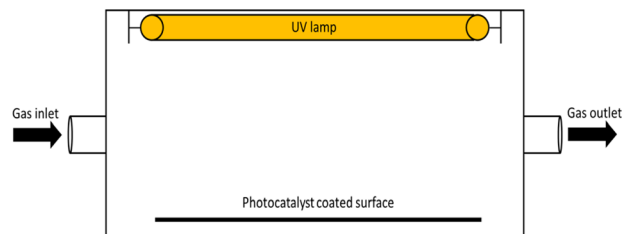
Fig. 9 Schematic of the reaction chamber.

UV, Jacksonville, FL) was mounted above the photocatalyst-coated glass and used to activate the photocatalyst for one hour. Nitrate washes were then performed and analyzed following the method mentioned above. This experimental setup deviates from the international standard (ISO 22197-1:2016 – Test method by using a larger photocatalytic reactor (56 Liters) which has an increased slit height (6 inches) and an increased reactor height (12 inches). This increases the residence time and distance of diffusion to the photocatalyst surface of gas during continuous flow photocatalytic removal experiments.

Conclusions

The effectiveness of photocatalytic abatement of NO_x through TiO_2-coated solar panels was explored through proof-of-concept laboratory testing and field testing of TiO_2-coated glass panels. Two different TiO_2-based photocatalytic coatings were successfully applied to glass slides during proof-of-concept testing. In the batch flow testing experiments, we achieved promising NO_x removal, up to 36.9% removal, when using the FN1 coating in ambient air-relevant conditions. Field testing was conducted to determine the magnitude of removal of three different TiO_2-based coatings. The magnitude of removal was quantified by the amount of nitrate formed due to NO_x oxidation through photocatalysis. Through IC analysis of the nitrate formed due to the photocatalytic oxidation of NO_x to NO_3^-/HNO_3, it was shown that NO_x removal was achieved in environmental conditions, up to an average nitrate flux of 8.82 mg per m^2 per day. By calculating the maximum possible nitrate formed based on an average NO_x concentration, it was determined that removal is inhibited by insufficient mass transfer to the photocatalyst surface. When considering the large-scale application of the FN1 coating to the solar panel fleet of Arizona State University, this would result in approximately 672 kg of NO_2 being removed per year. This is equivalent to offsetting the emissions of roughly 750 cars for a year. Based on the scale-up calculations, TiO_2 coating of the solar cell cover glass would not be an effective method for large-scale air remediation. However, it may be useful for local air remediation in areas such as parking garages with elevated NO_x concentrations.

Data availability

The authors confirm that the data supporting this study's findings are available within this article and/or its ESI.†

Conflicts of interest

There are no conflicts to declare.

Acknowledgements

References

1 A. Blomberg, M. T. Krishna, R. Helleday, M. Söderberg, M.-C. Ledin, F. J. Kelly, A. J. Frew, S. T. Holgate and T. Sandström, *Am. J. Respir. Crit. Care Med.*, 1999, **159**, 536–543.

2 R. J. Delfino, N. Staimer, T. Tjoa, D. Gillen, M. T. Kleinman, C. Sioutas and D. Cooper, *Environ. Health Perspect.*, 2008, **116**, 550–558.

3 U. Gehring, O. Gruzieva, R. M. Agius, R. Beelen, A. Custovic, J. Cyrys, M. Eeftens, C. Flexeder, E. Fuertes, J. Heinrich, B. Hoffmann, J. C. De Jongste, M. Kerkhof, C. Klümper, M. Korek, A. Mölter, E. S. Schultz, A. Simpson, D. Sugiri, M. Svartengren, A. Von Berg, A. H. Wijga, G. Pershagen and B. Brunekreef, *Environ. Health Perspect.*, 2013, **121**, 1357–1364.

4 Y. Jiang, Y. Niu, Y. Xia, C. Liu, Z. Lin, W. Wang, Y. Ge, X. Lei, C. Wang, J. Cai, R. Chen and H. Kan, *Environ. Res.*, 2019, **177**, 108620.

5 X. Zeng, G. Tian, J. Zhu, F. Yang, R. Zhang, H. Li, Z. An, J. Li, J. Song, J. Jiang, D. Liu and W. Wu, *Environ. Health*, 2023, **22**, 14.

6 P. J. Crutzen, *Q. J. R. Meteorol. Soc.*, 1970, **96**, 320–325.

7 W. L. Chameides, *Geophys. Res. Lett.*, 1978, **5**, 17–20.

8 National Research Council, *Rethinking the Ozone Problem in Urban and Regional Air Pollution*, National Academy Press, Washington, D.C, 1991.

9 G. A. Bishop, D. H. Stedman, J. De La Garza Castro and F. J. Dávalos, *Environ. Sci. Technol.*, 1997, **31**, 3505–3510.

10 F. Zeng, J. Finke, D. Olsen, A. White and K. L. Hohn, *Chem. Eng. J.*, 2018, **352**, 389–404.

11 E. Kritsanaviparkporn, F. M. Baena-Moreno and T. R. Reina, *Chemistry*, 2021, **3**, 630–646.

12 M. Vantol, *J. Catal.*, 1991, **129**, 186–194.

13 R. Q. Long and R. T. Yang, *J. Catal.*, 1999, **188**, 332–339.

14 M. A. Gómez-García, V. Pitchon and A. Kiennemann, *Environ. Int.*, 2005, **31**, 445–467.

15 C. Peng, R. Yan, H. Peng, Y. Mi, J. Liang, W. Liu, X. Wang, G. Song, P. Wu and F. Liu, *J. Hazard. Mater.*, 2020, **385**, 121593.

16 S. Yasumura, Y. Qian, T. Kato, S. Mine, T. Toyao, Z. Maeno and K. Shimizu, *ACS Catal.*, 2022, **12**, 9983–9993.

17 B. J. Bloomer, J. W. Stehr, C. A. Piety, R. J. Salawitch and R. R. Dickerson, *Geophys. Res. Lett.*, 2009, **36**, 2009GL037308.

18 K. Li, L. Chen, F. Ying, S. J. White, C. Jang, X. Wu, X. Gao, S. Hong, J. Shen, M. Azzi and K. Cen, *Atmos. Res.*, 2017, **196**, 40–52.

19 Z. Syrek-Gerstenkorn, B. Syrek-Gerstenkorn and S. Paul, *Appl. Sci.*, 2024, **14**, 3292.

20 J. Ângelo, L. Andrade, L. M. Madeira and A. Mendes, *J. Environ. Manage.*, 2013, **129**, 522–539.

21 J. Lasek, Y.-H. Yu and J. C. S. Wu, *J. Photochem. Photobiol., C*, 2013, **14**, 29–52.

22 Y. Boyjoo, H. Sun, J. Liu, V. K. Pareek and S. Wang, *Chem. Eng. J.*, 2017, **310**, 537–559.

23 A. K. Priya, R. Suresh, P. S. Kumar, S. Rajendran, D.-V. N. Vo and M. Soto-Moscoso, *Chemosphere*, 2021, **284**, 131344.

24 J. S. Dalton, P. A. Janes, N. G. Jones, J. A. Nicholson, K. R. Hallam and G. C. Allen, *Environ. Pollut.*, 2002, **120**, 415–422.

25 Th. Maggos, J. G. Bartzis, M. Liakou and C. Gobin, *J. Hazard. Mater.*, 2007, **146**, 668–673.

26 M.-Z. Guo, T.-C. Ling and C. S. Poon, *Cem. Concr. Compos.*, 2017, **83**, 279–289.

27 Y. Huang, W. Ho, S. Lee, L. Zhang, G. Li and J. C. Yu, *Langmuir*, 2008, **24**, 3510–3516.

28 J. Ma, H. He and F. Liu, *Appl. Catal., B*, 2015, **179**, 21–28.

29 M. Kuppusamy, S.-W. Kim, K.-P. Lee, Y. J. Jo and W.-J. Kim, *Nanomaterials*, 2024, **14**, 136.

30 M. Kuppusamy, M. Passi, S. K. Sundaram, G. Vadivel, M. Rathinasamy, K.-P. Lee and W.-J. Kim, *J. Environ. Chem. Eng.*, 2024, **12**, 112801.

31 J. Ma, C. Wang and H. He, *Appl. Catal., B*, 2016, **184**, 28–34.

32 Y. Li, Y. Sun, W. Ho, Y. Zhang, H. Huang, Q. Cai and F. Dong, *Sci. Bull.*, 2018, **63**, 609–620.

33 M. Baudys, Š. Paušová, P. Praus, V. Brezová, D. Dvoranová, Z. Barbieriková and J. Krýsa, *Materials*, 2020, **13**, 3038.

34 Y. Sun, Z. Zhao, F. Dong and W. Zhang, *Phys. Chem. Chem. Phys.*, 2015, **17**, 10383–10390.

35 G. Zhu, S. Li, J. Gao, F. Zhang, C. Liu, Q. Wang and M. Hojamberdiev, *Appl. Surf. Sci.*, 2019, **493**, 913–925.

36 F. Chang, B. Lei, C. Yang, J. Wang and X. Hu, *Chem. Eng. J.*, 2021, **413**, 127443.

37 M. Anpo, M. Matsuoka, K. Hano, H. Mishima, T. Ono and H. Yamashita, *Korean J. Chem. Eng.*, 1997, **14**, 498–501.

38 T. Du, L. Ren, Y. Zhang, M. Cui, Y. Chao, Y. Ge, N. Liu, Y. An and C. Meng, *Colloids Surf., A*, 2022, **641**, 128587.

39 O. Carp, *Prog. Solid State Chem.*, 2004, **32**, 33–177.

40 H. Chen, C. E. Nanayakkara and V. H. Grassian, *Chem. Rev.*, 2012, **112**, 5919–5948.

41 S. Banerjee, D. D. Dionysiou and S. C. Pillai, *Appl. Catal., B*, 2015, **176–177**, 396–428.

42 M. N. Chong, B. Jin, C. W. K. Chow and C. Saint, *Water Res.*, 2010, **44**, 2997–3027.

43 H. A. Foster, I. B. Ditta, S. Varghese and A. Steele, *Appl. Microbiol. Biotechnol.*, 2011, **90**, 1847–1868.

44 L. Zhang, P. Li, Z. Gong and X. Li, *J. Hazard. Mater.*, 2008, **158**, 478–484.

45 S. Laufs, G. Burgeth, W. Duttlinger, R. Kurtenbach, M. Maban, C. Thomas, P. Wiesen and J. Kleffmann, *Atmos. Environ.*, 2010, **44**, 2341–2349.

46 C. Guo, X. Wu, M. Yan, Q. Dong, S. Yin, T. Sato and S. Liu, *Nanoscale*, 2013, **5**, 8184.

47 M. Gallus, V. Akylas, F. Barmpas, A. Beeldens, E. Boonen, A. Boréave, M. Cazaunau, H. Chen, V. Daële, J. F. Doussin, Y. Dupart, C. Gaimoz, C. George, B. Grosselin, H. Herrmann, S. Ifang, R. Kurtenbach, M. Maille, A. Mellouki, K. Miet, F. Mothes, N. Moussiopoulos, L. Poulain, R. Rabe, P. Zapf and J. Kleffmann, *Build. Sci.*, 2015, **84**, 125–133.

48 Q. Jiang, T. Qi, T. Yang and Y. Liu, *Build. Sci.*, 2019, **158**, 94–103.

49 X. Xie, C. Hao, Y. Huang and Z. Huang, *Sci. Total Environ.*, 2020, **724**, 138059.

50 G. Luo, H. Liu, W. Li and X. Lyu, *Nanomaterials*, 2020, **10**, 2088.

51 H. Si, M. Zhou, Y. Fang, J. He, L. Yang and F. Wang, *Constr. Build. Mater.*, 2021, **298**, 123835.

52 E. Boonen and A. Beeldens, *Coatings*, 2014, **4**, 553–573.

53 M. Chen and J.-W. Chu, *J. Cleaner Prod.*, 2011, **19**, 1266–1272.

54 P. J. Tulpule, V. Marano, S. Yurkovich and G. Rizzoni, *Appl. Energy*, 2013, **108**, 323–332.

55 A. Iringová and M. Kovačic, *Transp. Res. Procedia*, 2021, **55**, 1171–1179.

56 C. G. Samal, D. Gupta, R. Pathania, S. Mohan and R. Suresh, *Indoor Built Environ.*, 2013, **22**, 710–718.

57 M. Debia, M.-C. Trachy-Bourget, C. Beaudry, E. Neesham-Grenon, S. Perron and C. Lapointe, *Environ. Sci. Pollut. Res.*, 2017, **24**, 4655–4665.

58 A. Gonzalez, A. Boies, J. Swanson and D. Kittelson, *Int. J. Environ. Res. Public Health*, 2022, **19**, 15223.

59 J. R. Caron and B. Littmann, *IEEE J. Photovolt.*, 2013, **3**, 336–340.

60 R. Nahar Myyas, M. Al-Dabbasa, M. Tostado-Véliz and F. Jurado, *Sol. Energy*, 2022, **237**, 19–28.

61 E. Luévano-Hipólito and A. Martínez-de La Cruz, *Constr. Build. Mater.*, 2018, **174**, 302–309.

62 X. Huang, S. Han, W. Huang and X. Liu, *Chem. Soc. Rev.*, 2013, **42**, 173–201.

63 R. Dillert, A. Engel, J. Große, P. Lindner and D. W. Bahnemann, *Phys. Chem. Chem. Phys.*, 2013, **15**, 20876.

64 Y. Paz, Z. Luo, L. Rabenberg and A. Heller, *J. Mater. Res.*, 1995, **10**, 2842–2848.

65 Y. Lai, Y. Tang, J. Gong, D. Gong, L. Chi, C. Lin and Z. Chen, *J. Mater. Chem.*, 2012, **22**, 7420.

66 A. Syafiq, B. Vengadaesvaran, A. K. Pandey and N. A. Rahim, *J. Nanomater.*, 2018, **2018**, 1–10.

67 Z. Guo, Z. Zhu, Y. Liu, C. Wu, H. Tu, J. Wang and X. Su, *Materials*, 2021, **14**, 1367.

68 G. San Vicente, A. Morales and M. T. Gutiérrez, *Thin Solid Films*, 2002, **403–404**, 335–338.

69 M. Grazia Salvaggio, R. Passalacqua, S. Abate, S. Perathoner and G. Centi, *Chem. Eng. Trans.*, 2015, **43**, 745–750.

70 H. Al Bakri, W. Abu Elhaija and A. Al Zyoud, *Energy*, 2021, **223**, 119908.

71 C. Tao, X. Zou, K. Du, G. Zhou, H. Yan, X. Yuan and L. Zhang, *J. Alloys Compd.*, 2018, **747**, 43–49.

72 A. A. Ahmad, Q. M. Al-Bataineh, A. M. Alsaad, T. O. Samara and K. A. Al-izzy, *Phys. B*, 2020, **593**, 412263.

73 M. Xu, Y. Wang, J. Geng and D. Jing, *Chem. Eng. J.*, 2017, **307**, 181–188.

74 M. Bellardita, M. Addamo, A. Di Paola, G. Marcì, L. Palmisano, L. Cassar and M. Borsa, *J. Hazard. Mater.*, 2010, **174**, 707–713.

75 K. A. Lohse, D. Hope, R. Sponseller, J. O. Allen and N. B. Grimm, *Sci. Total Environ.*, 2008, **402**, 95–105.

76 Q. L. Yu, Y. Hendrix, S. Lorencik and H. J. H. Brouwers, *Build. Sci.*, 2018, **142**, 70–82.

77 J. Fernández-Pampillón, M. Palacios, L. Núñez, M. Pujadas, B. Sanchez, J. L. Santiago and A. Martilli, *Atmos. Environ.*, 2021, **251**, 118190.

78 S. Weon and W. Choi, *Environ. Sci. Technol.*, 2016, **50**, 2556–2563.

79 W. El-Alami, D. Garzón Sousa, J. M. Díaz González, C. Fernández Rodríguez, O. González Díaz, J. M. Doña Rodríguez, M. El Azzouzi and J. Araña, *Chem. Phys. Lett.*, 2017, **684**, 164–170.

80 R. Zouzelka and J. Rathousky, *Appl. Catal., B*, 2017, **217**, 466–476.

81 R. Tantra, A. Sikora, N. B. Hartmann, J. R. Sintes and K. N. Robinson, *Particuology*, 2015, **19**, 35–44.

82 A. B. Nienhauser, M. S. Ersan, Z. Lin, F. Perreault, P. Westerhoff and S. Garcia-Segura, *J. Environ. Chem. Eng.*, 2022, **10**, 107192.